Simple and Rapid High-Yield Synthesis of Sub-100 nm Nano-SiO$_2$·0.5H$_2$O Particles Based on Wollastonite

Xiaolong Chen [1],†, **Yutong Zheng** [2],†, **Yuzhi Jiang** [3], **Yaxiong Ji** [1], **Shifeng Wang** [4],* and **Fujia Yu** [1]

[1] College of Resources and Civil Engineering, Northeastern University, Shenyang 110004, China; chenxlong8@163.com or chenxiaolong@mail.neu.edu.cn (X.C.); kobejyx@126.com (Y.J.); yufujia@mail.neu.edu.cn (F.Y.)

[2] Shenzhen Middle School, Renmin North Road, No. 18 Shenzhong Street, Luohu District, Shenzhen 518000, China; zhengyutong8@163.com

[3] College of Materials Engineering, Shenyang Ligong University, Shenyang 110000, China; jiangyz8@163.com

[4] Department of Physics, College of Science, Tibet University, Lhasa 850000, China

* Correspondence: wsf@utibet.edu.cn

† These authors contributed equally to this work.

Abstract: Amorphous nano-SiO$_2$·nH$_2$O particles has drawn much attention in industrial applications because of the features of high purification, low density, large specific surface area, fine decentralization, good optical, and mechanical performances. However, the applications have been hindered by the exorbitant price and the serious agglomeration. In this work, using wollastonite as reactant, H$_2$SO$_4$ as solvent, and adding sodium dodecyl benzene sulfonate (SDBS) as surfactant, sub-100 nm amorphous nano-SiO$_2$·0.5H$_2$O particles with good dispersibility, controllable agglomeration, narrow size distribution, and high yield were prepared by a low-cost and simple chemical method. The prepared sphere-like amorphous nano-SiO$_2$·0.5H$_2$O particles with average diameter of 70 nm were absorbed by the SDBS on the surface. The reaction conditions were systematically studied and the optimal technologic condition of the preparation was also confirmed. The achievement had a great perspective for the industrialization of high-quality nano-SiO$_2$·nH$_2$O particles, which hold great promise for various applications, such as plasmonic and catalytic nanoparticles supporting, polymeric matrices strengthening, drug delivery, and adsorption processes.

Keywords: nano-SiO$_2$·0.5H$_2$O; wollastonite; H$_2$SO$_4$; sub-100 nm; controllable agglomeration; low-cost

1. Introduction

White carbon black (WCB), that is nano-SiO$_2$·nH$_2$O particles, is a kind of amorphous nonmetallic nanomaterial [1,2]. It performs remarkable capabilities such as reinforcing property, thickening property, thixotropy, dispersity, insulative, anti-sticking property and has abundant applications [3–5]. As the superior additive, WCB makes itself indispensable in many industry areas, such as rubber, plastics, medicines, paints, household chemicals, compound materials of macromolecule, electronic encapsulation materials and precise ceramic materials [6,7]. 70 % of WCB is used in rubber industry, acting as the optimal reinforcing filler [8,9]. WCB is also widely used in adhesive and light industry due to the properties of small particle size, high corrosion resistance, high abrasion resistance and excellent insulation [10–12]. The superior performances will be largely influenced by the particle size and surface properties. It is vital to find a suitable preparation method.

The well-known Stober method to prepare silica particles was introduced during the 1970s, and remains today the most widely used wet chemical approach to silica nanoparticles (NPs) [13,14].

High-quality SiO_2 spheres of ~120nm were synthesized through the Stober process, in which hydrolysis and condensation of precursor tetraethyl orthosilicate (TEOS) occurred. The prepared SiO_2 NPs were then decorated with metal nanoparticles, forming nanohybrid systems for surface-enhanced Raman spectroscopy (SERS) and catalytic applications [14,15]. SiO_2 is the main component of its hydrated form ($SiO_2 \cdot nH_2O$), in which nH_2O exists as a surface hydroxyl group.

In past years, the gas phase method, liquid precipitation method, and sol-gel method are the main preparation methods for nano-$SiO_2 \cdot nH_2O$ particles [1,16]. In the mid-19th century, vitresence silica was prepared by Ebelmnaand and Grhaam by the sol-gel method. Using silane halide, hydrogen and oxygen, the nano-$SiO_2 \cdot nH_2O$ particles were synthesized by the gas phase method [17]. The products possess high purity, moderate dispersivity, small particle size, and few surface hydroxyl groups. However, the produces are high-cost because the method is much complex and requires expensive equipment [18]. Using sodium silicate as reactant and sulphuric acid or hydrochloric acid as solvent, nano-$SiO_2 \cdot nH_2O$ particles were prepared by liquid precipitation method [19]. The use of acid in large doses and complex processes hindered their application yet. More methods were reported to promote the quality as well as reduce the cost in the past years, including replacing the cheaper silicon sources, changing solvents and adding modifiers [20–22]. For example, the reaction system of wollastonite and hydrochloric acid is commonly used to prepared WCB [23,24] However, the method of preparation high-quality nano-$SiO_2 \cdot nH_2O$ particles for industrialization with low-cost is still few [25].

In this work, high-quality amorphous nano-$SiO_2 \cdot 0.5H_2O$ particles with a ca. 100 % yields were prepared by a low-cost chemical method using wollastonite as reactant, H_2SO_4 as solvent and sodium dodecyl benzene sulfonate (SDBS) as modifier. The particle size, phase composition, morphology, surface functional group, and the thermal stability of the product were analyzed. The prepared amorphous nano-$SiO_2 \cdot 0.5H_2O$ particles were around globular with average diameter of 70 nm, on the surface of which absorbed with SDBS to control particle agglomeration. The reaction conditions were explored in detail. The results confirmed the optimal condition: the reaction temperature was 85 °C, the reaction time was 30 min, agitation speed was 700 rpm, $n(H_2SO_4):n(CaSiO_3) = 2:1$, the initial wollastonite slurry concentration was 4.0%, the addition of SDBS was 2%. The effort of using wollastonite as the cheap silicon source made the cost down. The by-product $CaSO_4$ could also help reduce the production cost because it is widely used as the green environmentally friendly material [26]. The novel preparation method provides a pathway to control the agglomeration and improve the dispersity of nano-$SiO_2 \cdot 0.5H_2O$ particles.

2. Materials and Methods

2.1. Materials

Wollastonite minerals ($SiO_2 \geq 47.00\%$, $CaO \geq 46.00\%$, Al_2O_3: 0.25 %, Fe_2O_3: 0.3 %) were purchased from Faku, Shenyang, China. SDBS (95% purity) and sodium dodecyl sulfate (SDS) (95% purity) were purchased from Sinopharm Chemical Reagent Co. (Shanghai, China). KH-550 (99% purity), sulfuric acid (95%–98% purity), sodium hydroxide (99% purity) were purchased from Xinhua Reagent (Shenyang, China). Deionized (DI) water was used in all the experimental procedures.

2.2. Synthesis of Nano-SiO₂·0.5H₂O Particles

Amorphous nano-$SiO_2 \cdot 0.5H_2O$ particles were prepared by the chemical precipitation method. Briefly, The $CaSiO_3$ slurry (4 wt.% in water) was prepared by mixing wollastonite and SDBS (wollastonite:SDBS = 100:2, *m/m*) into DI water in a 1000 mL four-port reactor (see Figure 1) at 85 °C by means of a thermostatic water bath. Under stirring, H_2SO_4 (0.34 mol/kg) was dropwise added into the slurry. Here, the molar ratio of H_2SO_4 to $CaSiO_3$ ($n(H_2SO_4):n(CaSiO_3)$) is 2:1. The solution was kept stirring until no sedimentation existed. After aging, the by-product $CaSO_4$ was filtered and the remaining H_2SiO_3 collosol was kept stirred (700 rpm) at 85 °C. Then NaOH was introduced to adjust the pH of the collosol. The reaction was kept 30 min under stirring when the pH value of the

collosol was 8. The conditions were hereafter referred as the standard set. After that, the amorphous nano-$SiO_2 \cdot 0.5H_2O$ particles were collected, treated through washing with DI water and vacuum filtration, and finally dried at 70 °C. The vacuum filtration was performed by an SHZ-D(III) circulating water vacuum pump with a negative pressure of 0.1 MPa, and filter papers with pore size of ~1 μm were utilized.

Figure 1. The experiment set-up of the $SiO_2 \cdot nH_2O$ nanoparticles synthesis.

2.3. Measurements

The particle size was measured by laser particle analyzer (LS900, Omec Instruments, Zhuhai, China). The morphology of the as-prepared nanoparticles was characterized by scanning electron microscopy (SEM), which was performed on a Hitachi S-3400N scanning electron microscope (Tokyo, Japan) with an accelerating voltage of 20 kV. Dispersion of nanoparticles was prepared by adding 0.2 g nanoparticles into 40 mL absolute ethyl alcohol in a 50 mL centrifuge tube and ultrasonicated for 30 minutes. Several drops of the dispersion were pipetted onto the surface of cleaned conducting silicon wafer and dried. Prior to the SEM characterization, a thin layer of gold was coated onto the specimens to conduct the charge. A JEM-2100HR transmission electron microscope (TEM, JEOL, Tokyo, Japan) operating at 200 kV was employed to examine the microstructure and particle size of the prepared $SiO_2 \cdot nH_2O$ NPs. One drop of the pre-dispersed suspension was pipetted onto a carbon-coated grid, then the grid was placed on a Whatman paper to remove the solvent and naturally dried [27]. The crystal phase of the NPs was studied by using X-ray diffraction (XRD) (Ultima IV, Rigaku, Tokyo, Japan). Fourier transform infrared (FT-IR) spectra was obtained with FT-IR spectrometer (Avatar-380, Thermo-Nicolet, Waltham, MA, USA). The thermostability was analyzed by thermal gravimetric-differential scanning calorimeter (TG-DSC) thermal analyzer (SDT2960, TA, New Castle, DE, USA). The chemical composition of the product was characterized by using an energy dispersive spectrometer (EDS), which is attached to a JEOL 6490 microscope (Tokyo, Japan).

3. Results and Discussions

The nano-$SiO_2 \cdot 0.5H_2O$ particles were characterized when prepared at the standard conditions. Herein, the influence factors of the preparation were discussed, including the concentration of reactants, the reaction conditions. Since the performances of nano-$SiO_2 \cdot 0.5H_2O$ particles will be largely influenced

by the particle size, the average diameter of particles obtained by laser particle analyzer was used to evaluate the quality of productions under different conditions.

Briefly, the nano-SiO$_2$·0.5H$_2$O particles were prepared under the rule of the following reaction formula: CaSiO$_3$ + H$_2$SO$_4$ → SiO$_2$(s) + CaSO$_4$(s) + H$_2$O. The amount of CaSiO$_3$ slurry, H$_2$SO$_4$ and NaOH (pH value of solution) would largely influence the size of particles. Figure 2a demonstrated demonstrates the influence of CaSiO$_3$ slurry on the average diameter of Nano-SiO$_2$·0.5H$_2$O particles with other reagents held at the standard conditions. The concentration of slurry ranged from 3.3 to 4.3 wt.% in water was explored. With the increase of the concentration of slurry, the average diameter decreased from micrometer to nanometer and to sub-100 nm at the 3.9–4.0 wt.%. Keeping on increasing the concentration, the average diameter increased instead. Further study showed that the concentration of 4.0 wt.% induced the minimum average diameter, as shown in Figure 2b. Within a limited range, as the concentration of CaSiO$_3$ increased, the nucleation rate of nano-SiO$_2$·0.5H$_2$O particles would be enhanced and the growth of core would be restricted, promoting the decrease of diameter. Similar to the concentration of slurry, with the increase of the concentration of H$_2$SO$_4$ (the molar ratio of H$_2$SO$_4$ to CaSiO$_3$), the average diameter decreased in the early stage and then increased with other reagents held at the standard conditions. At the condition of n(H$_2$SO$_4$):n(CaSiO$_3$) = 2:1, the average diameter of nano-SiO$_2$·0.5H$_2$O particles reach to the minimum (Figure 2c). The low molar ratio of H$_2$SO$_4$ to CaSiO$_3$ would induce noncomplete reaction while the high molar ratio would induce the increase of the growth rate of silicic acid sol particles, resulting in an increase of average diameter. The pH value of solution adjusted by the concentration of NaOH was also quite crucial. At the condition of pH < 7, the nucleation and then growth of SiO$_2$ was difficult. At the condition of pH > 8, the silicic acid sol was easily transformed to gel due to the instability. At the condition of pH = 8, the average diameter of nano-SiO$_2$·0.5H$_2$O particles reached the minimum with other reagents held at the standard conditions (Figure 2d).
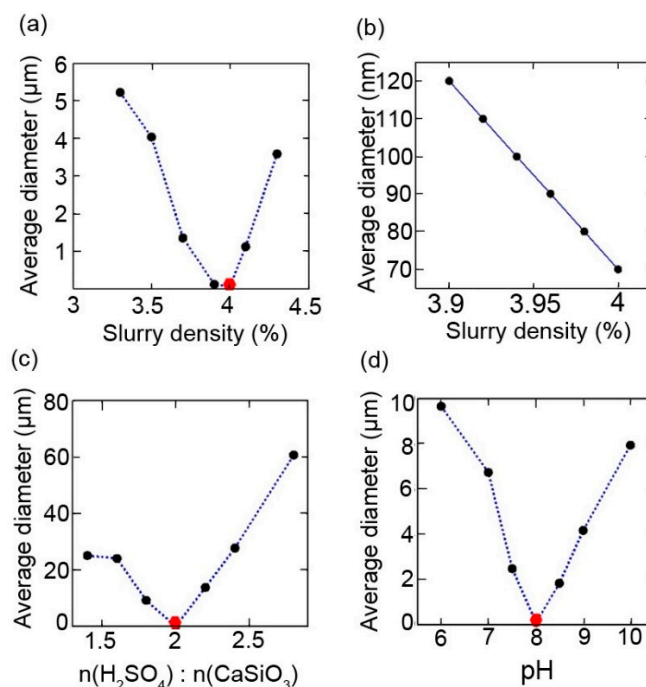

Figure 2. (**a**,**b**): The average diameter of nanoparticles with different concentrations of CaCO$_3$ slurry with other reagents held at the standard conditions. (**c**) The average diameter of nanoparticles with a different molar ratio of H$_2$SO$_4$ to CaSiO$_3$ with other reagents held at the standard conditions. (**d**) The average diameter of nanoparticles with different pH value with other reagents held at the standard conditions. The red hexagon indicated the average diameter of nanoparticles synthesized at the standard conditions. The average diameter at this point is 70 nm.

The reaction conditions (temperature, time and mixing speed) would also largely affect the size of nano-$SiO_2 \cdot 0.5H_2O$ particles. When the reaction temperature was below 70 °C, the low nucleation rate and high growth rate of SiO_2 and serious agglomeration made a large average diameter of particles. Increasing the temperature to more than 80 °C, the more drastic Brownian motion of colloid particles promote the formation of small particle size and the decrease of agglomeration. As shown in Figure 3a, when the reaction temperature is at 85 °C, the average diameter of nano-$SiO_2 \cdot 0.5H_2O$ particles reached the minimum with other reagents held at the standard conditions. It is important to give enough time for the reaction in order to achieve a complete reaction. For this study, when the reaction time was 30 min, the average diameter of nano-$SiO_2 \cdot 0.5H_2O$ particles reach to the minimum with other reagents held at the standard conditions, indicating to achieve the complete reaction (Figure 3b). Extending the reaction time, the average diameter increased due to the formation of clusters. Appropriate mixing speed also helps reduce the average diameter of productions. High mixing speed hinders the formation of silica sol while low mixing speed induces the formation of silica gel. As shown in Figure 3c, when the mixing speed is set to 700–900 rpm, the average diameter of nano-$SiO_2 \cdot 0.5H_2O$ particles reach to 100 nm with other reagents held at the standard conditions. Further study showed that the speed of 700 rpm induced the minimum average diameter (Figure 3d).
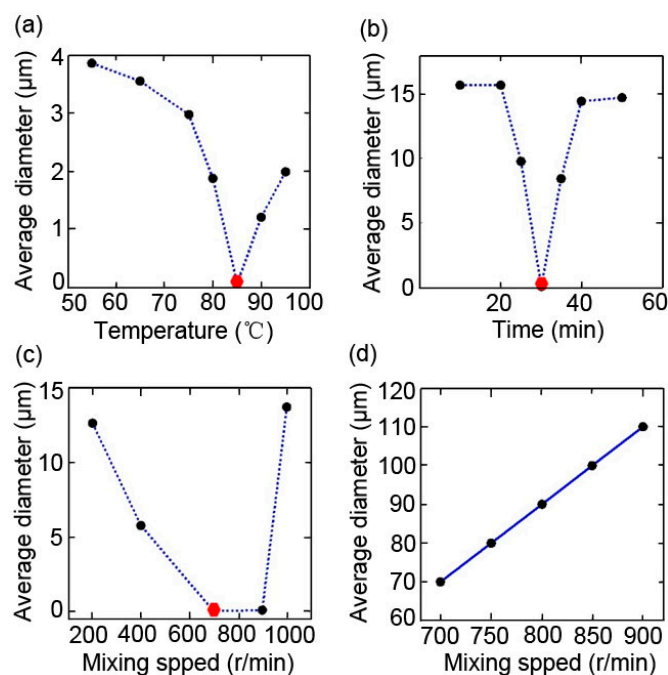

Figure 3. The average diameter of nano-$SiO_2 \cdot 0.5H_2O$ particles with the different (**a**) temperature, (**b**) time, (**c**,**d**) mixing speed with other reagents held at the standard conditions. The red hexagon indicated the average diameter of nanoparticles synthesized at the standard conditions. The average diameter at this point is 70 nm.

The addition of modifiers can help prevent the agglomeration and thus improve the dispersibility and stability of nanoparticles in the synthetic process. It also helps to reduce the average diameter of nanoparticles. In this work, the surfactant SDBS as the modifier was used to help reduce the average diameter of nano-$SiO_2 \cdot 0.5H_2O$ particles. In order to highlight the important effect of SDBS, SDBS was replaced by other surface modifiers like silane coupling agent (KH-550) and another surfactant (SDS) and the average diameter of productions were measured. Compared to the condition of no modifiers, all of them was benefited to reduce the average diameter. Without modifiers, the average diameter of production was 23 μm. The influence of concentration (dosage ratio) of SDBS on the average diameter was also explored.

The silane coupling agent is the most used surface modifiers for WCB. Absorbed in the surface of WCB via the formation of a chemical bond, the surface energy of particles will be decreased and thus the agglomeration will be largely reduced. KH-550 (silane coupling agent) was used to replace SDBS in the synthetic process. As shown in Figure 4a, with the dosage ratio of 3.5%, the average diameter of WCB particles reached 1.42 μm with other reagents held at the standard conditions. It is clearly demonstrated that the nanoscale WCB particles cannot be achieved according adding KH-550. The same phenomenon happened to SDS. Although the SDS can control the nucleation of WCB particles and their growth by releasing large amount of negative charge hydrophilic groups, the nanoscale WCB particles cannot be achieved. As shown in Figure 4b, with the dosage ratio of 0.5%, the average diameter of WCB particles reached 2.26 μm with other reagents held at the standard conditions. However, the use of SDBS can achieve nano-$SiO_2 \cdot 0.5H_2O$ particles. With the dosage ratio of 2%–2.4%, the WCB nanoparticles were obtained with other reagents held at the standard conditions. Further study showed that dosage ratio of 2 % induced the minimum average diameter (Figure 4c,d). The SDBS can contribute to improving the wettability of particles so that their stability can be improved [28–30]. The increase of anion group in the surface of particles due to the attachment of SDBS can enhance the electrostatic repulsion and the steric hindrance, thus the stability of particles can be improved [31–34]. As a result, the dispersibility of WCB particles can be improved and the size of WCB particles can be reduced.
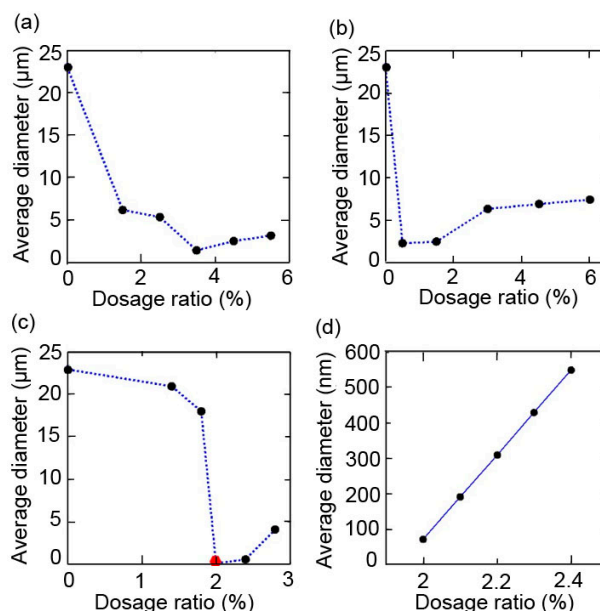

Figure 4. The average diameter of Nano-$SiO_2 \cdot 0.5H_2O$ particles with (**a**) KH-550, (**b**) SDS, (**c**) KH-550, (**c,d**) SDBS as a modifier with other reagents held at the standard conditions. The red hexagon indicated the average diameter of nanoparticles synthesized at the standard conditions. The average diameter at this point is 70 nm.

The nano-$SiO_2 \cdot 0.5H_2O$ particles were successfully synthesized and optimized through tailoring the preparation conditions. As shown in Figure 5a, the particle size of the optimized nano-$SiO_2 \cdot 0.5H_2O$ particles exhibits a narrow distribution, which ranges mainly between 55 and 110 nm and is centered on 70 nm. The gain diameter is less than 100 nm when the cumulative distribution reaches to 100% (see the insert of Figure 5a). TG-DSC curve, as shown in Figure 5b, demonstrates that the product possesses good thermostability as the residue rate is 83.09% at 900 °C. The FI-TR spectrum shows the characteristic peaks of WCB (475, 804, 960, 1107 cm^{-1}), H_2O (1633 cm^{-1}) and SDBS (1460 cm^{-1}), indicating the $SiO_2 \cdot nH_2O$ particles are indeed synthesized and coated with SDBS (Figure 5c) [35,36]. The XRD pattern in Figure 5d demonstrates that the particles are in the amorphous phase, and the broad peak located at about 22° indicates the formation of $SiO_2 \cdot 0.5H_2O$.
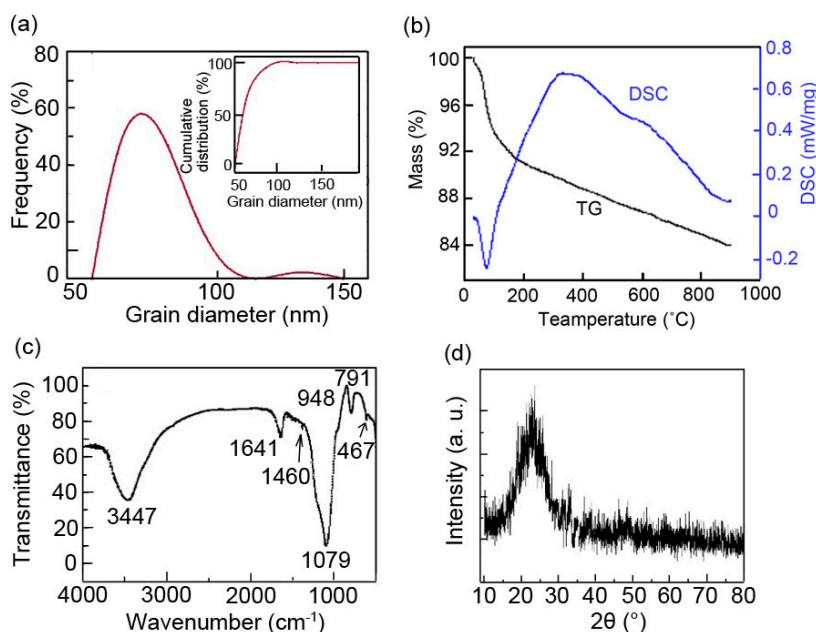
Figure 5. (**a**) The curve of the frequency distribution of nano-$SiO_2 \cdot 0.5H_2O$ particles. Insert: The curve of cumulative distribution of nano-$SiO_2 \cdot 0.5H_2O$ particles. (**b**) TG-DSC curve of Nano-$SiO_2 \cdot 0.5H_2O$ particles. The four peaks on DSC curve at 88.3, 321.2, 713.9 and 868.8 °C correspond to the weight loss rate of 2.72%, 9.53%, 0.75%, and 0.16%, respectively. The residue rate is 83.09 % at 900 °C. (**c**) The FT-IR spectrum of Nano-$SiO_2 \cdot 0.5H_2O$ particles. The peaks at 3447 cm^{-1} and 1641cm^{-1} are attributed to the O-H stretching vibration, while the peak at 1460 cm^{-1} is attributed to the CH_2-CH_2 scissoring vibration. The peak at 1079 cm^{-1} is attributed to the Si-O bending vibration, while the peak at 948 cm^{-1} is attributed to the Si-OH bending vibration, the peak at 791 cm^{-1} is attributed to the O-H bending vibration, and the peak at 467 cm^{-1} is attributed to the Si-O stretching vibration. (**d**) The XRD pattern of nano-$SiO_2 \cdot 0.5H_2O$ particles.

The microstructure and morphology of the prepared nano-$SiO_2 \cdot 0.5H_2O$ were investigated by using TEM and SEM, as shown in Figure 6. From the TEM image displayed in Figure 6a, it is seen that the prepared nano-$SiO_2 \cdot 0.5H_2O$ particles exhibit spherical shape with a diameter of approximately 70 nm, which is in excellent agreement with the particle size revealed by the laser particle analyzer as discussed above. The SEM image in Figure 6b also demonstrates that the average diameter of particles is less than 100 nm with few agglomerations, which is consistent with results from TEM and the laser particle analyzer.
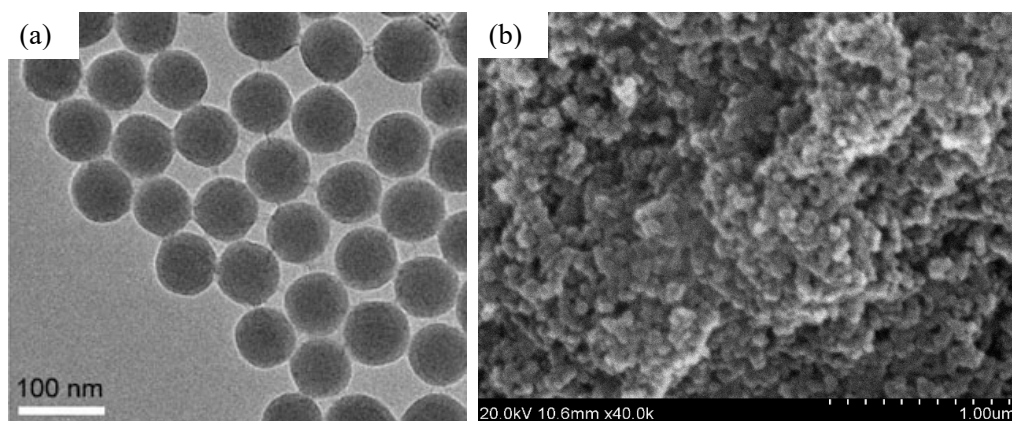

Figure 6. (**a**) TEM and (**b**) SEM image of nano-$SiO_2 \cdot 0.5H_2O$ particles.

To examine the chemical composition and purity of the prepared nano-$SiO_2 \cdot 0.5H_2O$ particles, EDS measurement was carried out, as shown in Table 1. It is obvious that the atomic ratio of Si to O in the samples is about 1:2.5, implying the formation of $SiO_2 \cdot 0.5H_2O$. The Na, S, and C elements are attributed to the SDBS surfactant, while the excess C is from the Carbon tape for fastening the samples in the vacuum chamber during the test. No other elements are detected, indicating the pure product of nano-$SiO_2 \cdot 0.5H_2O$ particles [37]. The EDS analysis is in good correspondence to the XRD identification and FT-IR findings.

Table 1. EDS analysis of the prepared nano-$SiO_2 \cdot 0.5H_2O$ particles.

Element	Weight %	Atomic %
C	18.15	26.35
O	48.63	52.94
Na	0.83	0.63
Si	31.47	19.58
S	0.92	0.5
Totals	100.00	

4. Conclusions

In conclusion, the effort of promoting the industrialized production of sub-100 nm amorphous $SiO_2 \cdot 0.5H_2O$ particles were reported. Using wollastonite as a reactant, H_2SO_4 as solvent and SDBS as a surfactant, the high-quality and high-yield nano-$SiO_2 \cdot 0.5H_2O$ particles with superior dispersibility and few agglomerations were synthesized by a simple and rapid chemical method. The optimal preparation conditions were demonstrated to be: the reaction temperature was 85 °C, the reaction time was 30 min, agitation speed was 700 rpm, $n(H_2SO_4):n(CaSiO_3) = 2:1$, the initial wollastonite slurry concentration was 4.0%, the addition of SDBS was 2%. The choose of wollastonite as silicon source can largely reduce the cost of preparation. The use of SDBS can greatly reduce the size and overcome the agglomeration of $SiO_2 \cdot 0.5H_2O$ particles. The simple, rapid and low-cost method had a great perspective for the industrialization of high-quality Nano-$SiO_2 \cdot 0.5H_2O$ particles and provide a frame of the preparation of WCB.

Author Contributions: Conceptualization, S.W.; methodology, X.C., Y.Z., Y.J. and S.W.; investigation, Y.Z., Y.J. and F.Y.; resources, F.Y.; data curation, X.C. and Y.J.; writing—original draft preparation, X.C. and Y.Z.; writing—review and editing, S.W.; supervision, Y.J. and S.W.

References

1. Luo, D.; Liu, J. Research progress on preparation of white carbon black from silicate ore. *Inorg. Chem. Ind.* **2008**, *2008*, 5.
2. Su, L.; Xie, J.; Xu, Y.; Wang, L.; Wang, Y.; Ren, M. Preparation and lithium storage performance of yolk-shell Si@void@C nanocomposites. *Phys. Chem. Chem. Phys.* **2015**, *17*, 17562–17565. [CrossRef] [PubMed]
3. Choi, S.-S.; Park, B.-H.; Song, H. Influence of filler type and content on properties of styrene-butadiene rubber (SBR) compound reinforced with carbon black or silica. *Polym. Adv. Technol.* **2004**, *15*, 122–127. [CrossRef]
4. Liu, B.; Sun, J.; Tan, G.; Liu, K.; Li, L.; Liu, Y. Effects of Nanometer Carbon Black on Performance of Low-Carbon MgO-C Composites. *J. Iron Steel Res. Int.* **2010**, *17*, 75–78. [CrossRef]
5. Shen, J.; Wang, H.; Zhou, Y.; Ye, N.; Wang, Y.; Wang, L. Hollow mesoporous frameworks without the annealing process for high-performance lithium–ion batteries: A case for anatase TiO_2. *Chem. Eng. J.* **2013**, *228*, 724–730. [CrossRef]

6.   Li, J.; Huang, J.; Zhao, J.; Qu, Y. Development status and market prospect of white carbon black. *Sci. Technol. Chem. Ind.* **2011**, *19*, 67–71.

7.   Jing, X. Status and Prospect of White Black Carbon from Non-metallic Minerals. *China Non-Met. Min. Ind. Her.* **2002**, *2002*, 5.

8.   Li, S.; Haiyan, Q. Preparation and application of white carbon black. *Inorg. Salt Ind.* **2008**, *40*, 8–11.

9.   He, Q.; Li, A.; Zhang, Y.; Liu, S.; Guo, Y.; Kong, L. A study on mechanical and tribological properties of silicone rubber reinforced with white carbon black. *Tribol. Mater. Surf. Interfaces* **2018**, *12*, 9–16. [CrossRef]

10.   Liu, D.-Z.; Fan, Z.-L.; Sun, P.-Q.; Dong, X.-R. Solution properties of chlorinated polypropylene and maleic anhydride grafted chlorinated polypropylene. *Phys. Chem. Liq.* **2004**, *42*, 551–560. [CrossRef]

11.   Wang, Z.; Zhang, Y.; Zhang, K.; Hu, G. Study on Non-isothermal Crystallization Kinetics of Polyamide 11/Silica Nanocomposites. *Eng. Plast. Appl.* **2012**, *40*, 70–73.

12.   Wang, Y.; Yang, H.; Xu, H. DNA-like dye-sensitized solar cells based on TiO_2 nanowire-covered nanotube bilayer film electrodes. *Mater. Lett.* **2010**, *64*, 164–166. [CrossRef]

13.   Stober, W.; Fink, A.; Bohn, E. Controlled Growth of Monodisperse Silica Spheres in the Micron Size Range. *J. Colloid Interface Sci.* **1968**, *26*, 62–69. [CrossRef]

14.   Tzounis, L.; Contreras-Caceres, R.; Schellkopf, L.; Jehnichen, D.; Fischer, D.; Cai, C.; Uhlmann, P.; Stamm, M. Controlled Growth of Ag Nanoparticles Decorated onto the Surface of SiO_2 Spheres: A Nanohybrid System with Combined SERS and Catalytic Properties. *RSC Adv.* **2014**, *4*, 17846–17855. [CrossRef]

15.   Tzounis, L.; Logothetidis, S. $Fe_3O_4@SiO_2$ Core Shell Particles as Platforms for the Decoration of Ag Nanoparticles. *Mater. Today Proc.* **2017**, *4*, 7076–7082. [CrossRef]

16.   Checmanowski, J.G.; Gluszek, J.; Masalski, J. Role of Nanosilica and Surfactants in preparation of SiO_2 coatings by sol-gel process. *Ochr. Przed Koroz.* **2002**, *11*, 214–218.

17.   Barthel, H.; Rösch, L.; Weis, J. Fumed Silica-Production, Properties, and Applications. In *Organosilicon Chemistry Set*; Wiley-VCH Verlag GmbH: Weinheim, Germany, 1996; pp. 761–778.

18.   Wang, Y.; Yang, H.; Liu, Y.; Wang, H.; Shen, H.; Yan, J.; Xu, H. The use of Ti meshes with self-organized TiO_2 nanotubes as photoanodes of all-Ti dye-sensitized solar cells. *Prog. Photovolt. Res. Appl.* **2010**, *18*, 285–290.

19.   Jesionowski, T. Preparation of spherical silica in emulsion systems using the co-precipitation technique. *Mater. Chem. Phys.* **2009**, *113*, 839–849. [CrossRef]

20.   Nandiyanto, A.B.D.; Kim, S.-G.; Iskandar, F.; Okuyama, K. Synthesis of spherical mesoporous silica nanoparticles with nanometer-size controllable pores and outer diameters. *Microporous Mesoporous Mater.* **2009**, *120*, 447–453. [CrossRef]

21.   Xu, K.; Sun, Q.; Guo, Y.; Zhang, Y.; Dong, S. Preparation of super-hydrophobic white carbon black from nano-rice husk ash. *Res. Chem. Intermed.* **2014**, *40*, 1965–1973. [CrossRef]

22.   Khan, M.; Saha, M.; Sultana, S.; Ahmed, A. Preparation and Characterization of White Carbon Black from Rice Husk. *J. Environ. Sci. Nat. Resour.* **2017**, *9*, 1–7. [CrossRef]

23.   Zhen, L.; Keqin, C. Experimental research on the preparation of white carbon black by acid treatment of wollastonite. *Conserv. Utili. Mineral. Resources* **1999**, *1*, 18–20.

24.   Chunsheng, L. To Analyze the Principle of Reaction and the Kinetics of Preparing Silica from Wollastonite. *China Non-Met. Min. Ind. Her.* **2006**, *55*, 32–35.

25.   Yang, C.M.; Cho, A.T.; Pan, F.M.; Tsai, T.G.; Chao, K.J. Spin-on Mesoporous Silica Films with Ultralow Dielectric Constants, Ordered Pore Structures, and Hydrophobic Surfaces. *Adv. Mater.* **2001**, *13*, 1099–1102. [CrossRef]

26.   Wang, H.; Liu, G.; Huang, J.; Zhou, Y.; Yao, Q.; Ma, S.; Cao, K.; Liu, Y.; Wu, W.; Sun, W.; et al. Performance of an environmentally friendly anti-scalant in $CaSO_4$ scale inhibition. *Desalin. Water Treat.* **2015**, *53*, 8–14. [CrossRef]

27.   Tzounis, L.; Kirsten, M.; Simon, F.; Mader, E.; Stamm, M. The Interphase Microstructure and Electrical Properties of Glass Fibers Covalently and Non-covalently Bonded with Multiwall Carbon Nanotubes. *Carbon* **2014**, *73*, 310–324. [CrossRef]

28.   Bi, Z.; Zhang, Z.; Xu, F.; Qian, Y.; Yu, J. Wettability, Oil Recovery, and Interfacial Tension with an SDBS–Dodecane–Kaolin System. *J. Colloid Interface Sci.* **1999**, *214*, 368–372. [CrossRef]

29.   Wang, B.-X.; Zhao, Y.; Zhao, X.-P. The wettability, size effect and electrorheological activity of modified titanium oxide nanoparticles. *Coll. Surfaces A Physicochem. Eng. Asp.* **2007**, *295*, 27–33. [CrossRef]

30. Gu, C.; Zhang, J.; Tu, J. A strategy of fast reversible wettability changes of WO_3 surfaces between superhydrophilicity and superhydrophobicity. *J. Colloid Interface Sci.* **2010**, *352*, 573–579. [CrossRef]

31. Wang, X.-J.; Zhu, D.-S.; Yang, S. Investigation of pH and SDBS on enhancement of thermal conductivity in nanofluids. *Chem. Phys. Lett.* **2009**, *470*, 107–111. [CrossRef]

32. Park, S.; Ruoff, R.S. Chemical methods for the production of graphenes. *Nat. Nanotechnol.* **2009**, *4*, 217–224. [CrossRef] [PubMed]

33. Zinatloo-Ajabshir, S.; Mortazavi-Derazkola, S.; Salavati-Niasari, M. Nd_2O_3 nanostructures: Simple synthesis, characterization and its photocatalytic degradation of methylene blue. *J. Mol. Liq.* **2017**, *234*, 430–436. [CrossRef]

34. Su, L.; Jiang, J.; Wang, L.; Wang, Y.; Ren, M. MnO QD/Graphene Dot Fabrics: A Versatile Nanohybrid Material. *ChemElectroChem* **2015**, *2*, 789–794. [CrossRef]

35. Tan, X.; Fang, M.; Chen, C.; Yu, S.; Wang, X. Counterion effects of nickel and sodium dodecylbenzene sulfonate adsorption to multiwalled carbon nanotubes in aqueous solution. *Carbon* **2008**, *46*, 1741–1750. [CrossRef]

36. Du, Y.; Du, X.; George, S.M. Mechanism of Pyridine-Catalyzed SiO_2 Atomic Layer Deposition Studied by Fourier Transform Infrared Spectroscopy. *J. Phys. Chem. C* **2007**, *111*, 219–226. [CrossRef]

37. Wang, Y.; Liu, Y.; Yang, H.; Wang, H.; Shen, H.; Li, M.; Yan, J. An investigation of DNA-like structured dye-sensitized solar cells. *Curr. Appl. Phys.* **2010**, *10*, 119–123. [CrossRef]